

Muon Polarization and Energy Spectrum in $K^+ \rightarrow \pi^0 + \mu^+ + \nu$ †

D. CUTTS, T. ELIOFF, AND R. STIENING

Lawrence Radiation Laboratory, University of California, Berkeley, California

(Received 15 January 1965)

The number of muons in the high-energy region of the continuum in the reaction $K^+ \rightarrow \pi^0 + \mu^+ + \nu$ has been measured. The portion of the spectrum explored extended from 107.1 to 126.4 MeV. We measured the longitudinal polarization of the muons in the same energy interval by observing the spatial anisotropy of the e^+ from muon decay. The rate of decay with a muon in this energy interval was found to be 0.054 ± 0.008 of the total K^+ decay rate in the mode $K^+ \rightarrow \pi^0 + e^+ + \nu$. The polarization of the muons was found to be $+0.61 \pm 0.39$. These results are consistent with an analysis made assuming constant form factors, pure vector coupling, and equal muon and electron weak-coupling strength. A real or imaginary vector form-factor ratio, $\xi = f_-/f_+$, is consistent with the data. If ξ is real, the most probable solution is $+0.2 < \xi < +1.4$. As a calibration experiment, we measured the polarization of muons from $K^+ \rightarrow \mu^+ + \nu$. We found it to be -0.94 ± 0.21 .

INTRODUCTION

THE central idea of the present theory of weak interactions is that the Hamiltonian density can be written as the product of a current with itself:

$$H = \sum_{\lambda} J_{\lambda}^* J_{\lambda}. \quad (1)$$

The current J_{λ} is thought of as being the sum of a number of contributions;

$$J_{\lambda} = J_{\lambda}^l + J_{\lambda}^{s, \Delta s=0} + J_{\lambda}^{s, \Delta s=1} + \dots \quad (2)$$

In this picture the various observed weak processes arise from different terms in the product $\sum J^* J$.

From nuclear beta decay, muon decay, and pion decay, the structure of the leptonic-current term in the above sum has been established as

$$J_{\lambda}^l = (G/\sqrt{2}) [\bar{U}_{\mu} \gamma_{\lambda} (1 + \gamma_5) U_{\nu, \mu} + \bar{U}_e \gamma_{\lambda} (1 + \gamma_5) U_{\nu, e}]. \quad (3)$$

It is essential to the above theory that the form of J_{λ}^l be that given above in all processes in which J_{λ}^l appears. One test of this is the coupling of J_{λ}^l to the current of strongly interacting particles which changes strangeness, $J_{\lambda}^{s, \Delta s=1}$. It is known that weak decays which change strangeness are slower than those which do not change strangeness. The question then arises whether the structure of the weak coupling is different in the processes which change strangeness.

The process that has been chosen to study this coupling is the $K^+ \rightarrow \pi^0 + \mu^+ + \nu$ decay. By measuring the energy spectrum as well as the polarization of the muons, one can determine the structure of the muonic part of the weak current J_{λ}^l . Furthermore, by comparing the process with the $K^+ \rightarrow \pi^0 + e^+ + \nu$ decay it is possible to test the equality of coupling strength of electrons and muons which is implied by the form of J_{λ}^l .

EXPERIMENTAL ARRANGEMENT

A. K^+ Meson Beam

The K^+ source was obtained by degrading to rest the K^+ mesons in an unseparated, momentum-analyzed secondary-particle beam produced when 5.2-BeV protons struck a three-inch thick uranium target.¹ The magnet system used for the momentum analysis of the secondary beam is shown in Fig. 1. Particles produced in a direction parallel to the incident proton beam were deflected through an angle of 35° by magnet B1. A quadrupole doublet Q1, Q2 with Q1 focusing in the horizontal plane, focused the beam on the stopping region. Magnet B2 deflected the beam through another angle of 35° . The beam was collimated at the entrance and exit of the quadrupole doublet and in the bending magnet B2. In order to compensate for the momentum dispersion of the beam at the stopping region, part of

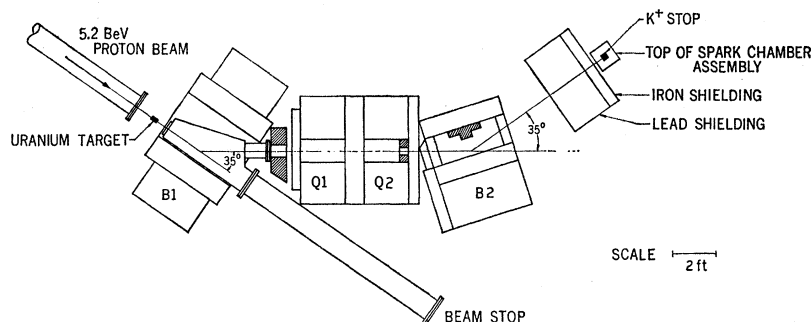


FIG. 1. Magnet system of 470-MeV/c unseparated K^+ beam.

† Work performed under the auspices of the U. S. Atomic Energy Commission.

¹ Preliminary results of this experiment are given in the Bull. Am. Phys. Soc. 10, 91 (1965).

the carbon degrader used to stop the K^+ mesons was wedge-shaped. We used a counter system to separate stopping K^+ mesons from other particles in the beam. It consisted of three scintillation counters, S2, S3, and S4, in the beam degrader, with discriminators set to require pulses greater than those produced by minimum ionizing particles, and a water Čerenkov counter in anticoincidence to reject fast particles. There were two scintillation counters, S6 and S6B, in which the K^+ mesons stopped, and a scintillation counter S7 in anticoincidence to reject particles passing through the entire telescope.

The rate at which K^+ mesons could be stopped was limited by the background in the spark chambers caused by the interactions of π^+ mesons in the beam with the degrader. The momentum of the beam was set to maximize the ratio of stopping K^+ mesons to π^+ mesons passing through the degrader. The momentum chosen as optimum with regard to this consideration was 470 MeV/ c . In the experiment the stopping K^+ rate was about 800 particles/Bevatron pulse. Under these conditions, the π^+ rate in the counter telescope was about 400 000/pulse. The average Bevatron pulse duration was 0.6 seconds.

B. Spark Chambers and Counters

Figure 2 shows the apparatus used to detect K^+ decays. An acceptable event occurred when a K^+ came to rest in either counter S6 or S6B and decayed, giving rise to a μ^+ lepton which passed through the T2, T3, T4 counter telescope and came to rest before reaching anticoincidence counter T5. Between T2 and T4 spark chambers with copper plates degraded the muons, and permitted observation of their behavior during the degrading process. Between T4 and T5, spark chambers with plates made of 20% aluminum and 80% carbon ($\rho=1.76$) were operated so as to be sensitive to both the stopping muon and to the positron from the muon decay provided that the decay occurred within 3.3×10^{-6} seconds after the muon stopped. We measured the longitudinal polarization of the stopping muons by observing the spatial distribution of the positrons in the $\mu^+ \rightarrow e^+ + \nu + \bar{\nu}$ decays. We measured the energy distribution of the muons from K^+ decay by observing the range distribution of the muon-decay vertices, or the stopping points when a decay positron was not visible. We determined the branching ratio for $K^+ \rightarrow \pi^0 + \mu^+ + \nu$ with muons in the above range interval by comparing the number of stopping muons with the number of T2, T3, T4, T5 coincidences. These later events were almost entirely due to muons from $K^+ \rightarrow \mu^+ + \nu$ events.

The range interval between T4 and T5 in which the muons came to rest was selected to be beyond the range of π^+ mesons from the decay $K^+ \rightarrow \pi^0 + \pi^+$, but less than the range of muons from the decay $K^+ \rightarrow \mu^+ + \nu$. The muon kinetic energy corresponding to the chosen range interval extended from 107 to 135 MeV. Because the

rate of muons from $K^+ \rightarrow \pi^0 + \mu^+ + \nu$ was small compared to other backgrounds near the high end of the range interval, only those muons with an initial kinetic energy of less than 126.4 MeV were used in the data analysis. In addition to muons from $K^+ \rightarrow \pi^0 + \mu^+ + \nu$, other K^+ decay processes can give rise to particles stopping in the above described range interval.

These are

- (1) muons from $K^+ \rightarrow \mu^+ + \nu + \gamma$;
- (2) muons from the decay in flight of pions from $K^+ \rightarrow \pi^0 + \pi^+$;
- (3) the decay in flight of muons from $K^+ \rightarrow \mu^+ + \nu$;
- (4) muons and pions from the decay in flight of K^+ mesons in the region of the S6, S6B stopping counters;
- (5) positrons from $K^+ \rightarrow \pi^0 + e^+ + \nu$;
- (6) particles from K^+ mesons which came to rest at positions not in the S6 and S6B stopping counters.

The first three categories of background events could not be distinguished from $K^+ \rightarrow \pi^0 + \mu^+ + \nu$ events since π^0 -decay gamma rays were not detected. We have accounted for the events in these categories by calculations taking into account the K^+ -decay branching ratios and the geometry of the spark-chamber assembly. These calculations will be described later. Background events in the remaining three categories were eliminated by making use of the pulse-height and time information from the scintillation counters, and by conditions set on the appearance of particle tracks in the spark chambers.

We utilized the pulse-height and time information from the scintillation counters in the following manner: A stopping K^+ was identified as a coincidence among counters S3, S4, S5, and S6 in anticoincidence with a water Čerenkov counter and counter S7. Pulses were accepted from S3, S4, S5, and S6 only if the pulse height was considerably greater than that corresponding to a minimum ionizing particle. The pulse-height condition on S6 was such that the minimum acceptable energy loss was 6 MeV, or more than twice the energy loss of a minimum ionizing particle. When the K^+ penetrated the S6B counter, the information was used to light a marker lamp which appeared on the spark-chamber photograph if a picture was taken. This was done so that a range correction could be applied to the K^+ decay products. These criteria on the stopping K^+ beam were sufficient to eliminate most of the other particles in the unseparated beam. The background of events satisfying the above conditions but not due to stopping K^+ mesons was less than 10% of the stopping K^+ rate.

Whenever the K^+ beam-counter telescope indicated that a K^+ had stopped, a gate was opened to accept a coincidence in the T2, T3, T4 counter telescope provided that it occurred after a certain time delay. This delay was chosen to provide good rejection of events due to K^+ decay in flight. This is important because K^+ decays in flight in the mode $K^+ \rightarrow \pi^+ + \pi^0$, with the π^+ going slightly forward in the center-of-mass system, would

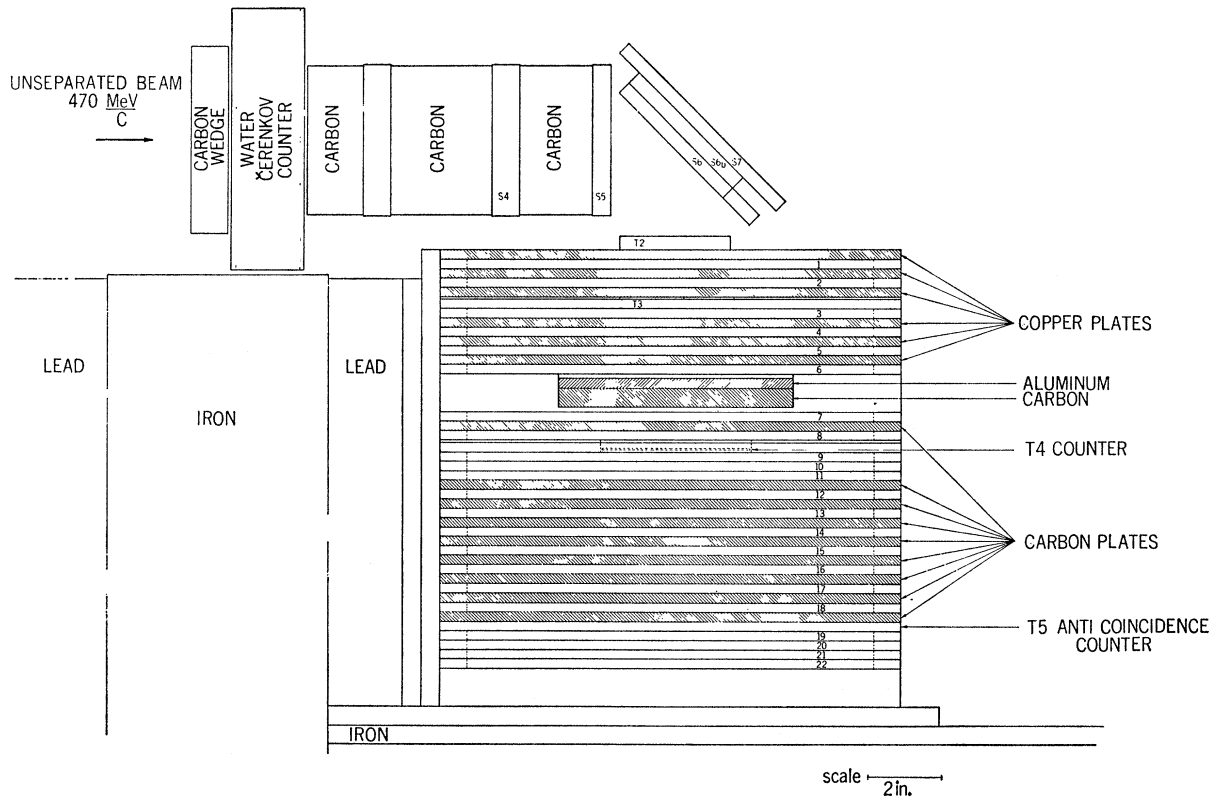


FIG. 2. Side view of spark-chamber assembly. The unseparated beam passes through the counter telescope at the top of the assembly. K^+ mesons stop in the counters numbered S6 and S6B.

have been a considerable background. The minimum time delay between a K^+ stop and the observation of a decay product was set at 6×10^{-9} seconds. To determine the rejection rate of prompt events that such a delay implies, the K^+ telescope was set to accept π^+ mesons. Charge exchange and scattering in S6 provided a convenient source of prompt events. The rejection rate of prompt events at the minimum delay time of 6×10^{-9} seconds was at least 200:1. This condition rendered negligible the background of K^+ decay in flight in the stopping counters. The delay time interval in which K^+ decays were accepted extended about 25×10^{-9} seconds beyond the minimum acceptable delay time.

In addition to the time-delay condition set on the K^+ decay muon, pulse-height criteria were applied to the T2, T3, and T4 scintillation counters. In each of the counters, the minimum pulse-height condition was set so that the efficiency for detecting muons from $K^+ \rightarrow \mu^+ + \nu$ was greater than 95%. The efficiency for detecting stopping muons from $K^+ \rightarrow \pi^0 + \mu^+ + \nu$ was therefore also greater than 95%. In addition to these lower limits on the pulse height, an upper limit was set on counter T2 so that events would not be detected in which a scattered K^+ meson stopped at an appreciable depth in T2 and decayed in a manner which simulated a decay originating from a K^+ stop in S6 or S6B. This

condition had a negligible effect on the $K^+ \rightarrow \pi^0 + \mu^+ + \nu$ rate. Whenever the pulse height in the T4 counter was high enough to indicate that a muon had stopped in the counter, the information was displayed on the spark-chamber photograph in the form of a marker lamp. Since muons stopping in a plastic scintillator are depolarized,² it was necessary to reject such events. This was done by rejecting all events in which the muon-decay vertex appeared in the region of the T4 counter. The marker-lamp information indicated that the rejection had been made correctly. Because the T4 counter was only $\frac{1}{16}$ in. thick, the number of events rejected was not large.

It was necessary that the T5 anticoincidence counter be very efficient. For every muon that stopped between T4 and T5 from $K^+ \rightarrow \pi^0 + \mu^+ + \nu$, about 250 muons from $K^+ \rightarrow \mu^+ + \nu$ passed through the stopping region and the anticoincidence counter. Any event not rejected by the anticoincidence counter would be identified as a forward $\mu \rightarrow e^+ + \nu + \bar{\nu}$ decay. In order to insure that the anticoincidence counter was efficient, it was dc coupled to the coincidence circuit. To determine that the counter was effective, we took a sample of photographs of the spark chambers in which the chambers normally re-

² R. Swanson, Phys. Rev. 112, 580 (1958).

vealing the muon decay were pulsed without the usual 3.3×10^{-6} -sec time delay. In this case the delay time was 0.34×10^{-6} sec. The number of muon decays visible in the forward direction through the T5 counter decreased in accordance with the expectation based on the muon lifetime. A certain number of stopping muons decayed in the forward direction within 10^{-8} seconds after stopping. These were also rejected by the T5 counter. A small correction was made to the data to account for this loss. The loss of events caused by the T5 anticoincidence counter detecting the showers from the π^0 -decay gamma rays was computed by a Monte Carlo technique. The loss was less than 1% of the events.

Throughout the experiment, a scaler recorded the events occurring subject to the same conditions as the $K^+ \rightarrow \pi^0 + \mu^+ + \nu$ events except that the T5 counter was in coincidence rather than anticoincidence. By scanning a sample of pictures which were taken with the spark chambers triggered by this scaler signal, it was established that 0.992 of these events were caused by muons from $K^+ \rightarrow \mu^+ + \nu$.

The spark chambers were not all operated under the same conditions. The chambers numbered 1 to 6 in Fig. 2 were separated by 0.25-in. thick copper plates and were pulsed 340×10^{-9} sec after the passage of a particle through the T2, T3, T4 counter telescope. There was a 40-V clearing potential applied to these chambers to keep the resolving time short. The spark chambers numbered from 7 to 22 were operated with a 4-V clearing potential and were pulsed 3.3×10^{-6} seconds after the passage of a particle through the counter telescope. Although the quality of the tracks in this section of spark chambers was not good because of the difference in ionization between the stopping muons and the decay positrons, and the difference in time between the passage of the particles, tracks were always visible. Frequently some of the sparks were, however, very weak. Both sets of spark chambers were filled with a 90% neon, 10% helium mixture, and were photographed with a lens opening of f 5.6 using Tri-X film.

The chance background rate in the spark chambers due to pions in the unseparated beam interacting in the K^+ degrader was such that there were frequently background tracks in the spark chambers in which the muon decays were observed. In these cases, the track in the short resolving-time region of the spark chambers tagged the K^+ decay event. The number of events that were lost because background tracks overloaded the muon decay spark chambers was negligible.

In scanning the photographs, we accepted only those events in which the appearance of the particle track in the short resolving time region of the spark chambers was satisfactory, i.e., we required that there be no sparks missing in the track, and that there be no other sparks within 1 cm of the track. Furthermore, events which showed a single scatter of more than 20° were rejected. These conditions were used to reject positrons. The

scanning loss of muon events was determined by applying the above conditions to a sample of muons from $K^+ \rightarrow \mu^+ + \nu$ which were known to be uncontaminated with positrons. The scanning efficiency measured with these events was 0.92 ± 0.01 . A correction for this loss of muon events was made in the data analysis. In the sample of otherwise acceptable $K^+ \rightarrow \pi^0 + \mu^+ + \nu$ events, 12% of the events violated one of the above scanning conditions. Since we expected a loss of 8% because of the spark chamber inefficiency as measured with the $K^+ \rightarrow \mu^+ + \nu$ events, we assumed that the remaining 4% are positrons. This assumption is supported by the observation that the rejected events did not show as many decay vertices as would have been expected from muon decays.

C. Muon Range-Determination Procedure

The energy of a stopping muon was determined from its range. In the range measurement we took into account the depth in the S6, S6B stopping region at which the K^+ decay took place, and the angle of incidence of the muon on the spark-chamber plates. The analysis procedure is as follows. The range of the muon was assigned a bin number equal to the number of the last spark chamber in which the muon was visible. If the S6B marker lamp indicated that the K^+ had stopped in S6B, the bin number was increased by one in order to account for the energy loss of the muon in crossing counter S6. The counter thickness was chosen to be equivalent to one spark-chamber plate. The angle between the normal to the spark-chamber plates and the path of the muon as it crossed the first two spark chambers after leaving the K^+ stopper was measured in each event. If this angle was between 14.5 and 20.5° , the bin number was increased by one. If the angle was between 20.5 and 24.5° , the bin number was increased by two. Events with a total correction of more than two bins were rejected.

To determine the average initial kinetic energy corresponding to the various bins after making the corrections described above, a small amount of degrader was removed from the spark chambers in order that pions from the decay $K^+ \rightarrow \pi^+ + \pi^0$ would stop in the carbon-plate region. The bin distribution of these events is shown in Fig. 3. The range-energy tables of Sternheimer³ were used to derive from this observed pion range the energy of a muon with the same range, and to account for the small amount of additional degrader used in the muon experiment. A similar procedure was applied to compute the bin energy from the distribution of stopping muons from $K^+ \rightarrow \mu^+ + \nu$. The energy scales computed by these two different procedures differed by 1.7 MeV. An average of the two has been chosen. An absolute

³R. M. Sternheimer in *Techniques of High Energy Physics*, edited by D. Ritson (Interscience Publishers, Inc., New York, 1961), Appendix V.

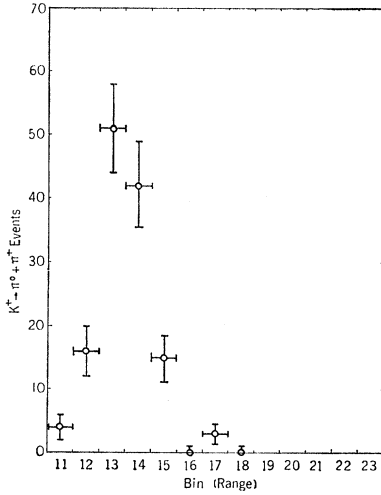


FIG. 3. Range distribution of π^+ mesons from $K^+ \rightarrow \pi^0 + \pi^+$. Part of the degrader in the spark-chamber assembly has been removed to permit this measurement.

error in energy scale of one bin or ± 2.75 MeV has been assumed in the data analysis. The energy resolution function shown in Fig. 3 caused a negligible distortion of the muon spectrum in $K^+ \rightarrow \pi^0 + \mu^+ + \nu$.

DATA ANALYSIS

A. Decay-Rate Measurement

The efficiency for detecting particles was a function of the range. This variation in efficiency was caused by two factors: (1) The varying angle of incidence of the muons on the spark-chamber plates, and (2) the varying depth in the K^+ stopping counters at which the muons originated. The first range interval in which the muons could stop and be detected (No. 11) contained only those events in which the K^+ stopped in S6 and the deviation of the muon from normal incidence on the spark chamber plates was less than 14.5° . On the other hand, in range interval No. 15, the events could come from K^+ stops in S6 or S6B, and from a variety of incidence angles. Since the scaler counting muons from

$K^+ \rightarrow \mu^+ + \nu$ was sensitive to all K^+ decays because the T5 counter was much larger than the solid angle subtended by the T3, T3, T4 telescope, it was necessary to determine the efficiency for detecting stopping muons. To determine the efficiency $S(j)$ for detecting particles stopping in range interval j after the various corrections, additional degrader was added to the spark chambers in order that muons from $K^+ \rightarrow \mu^+ + \nu$ stopped in the center of the carbon plate region. The number of events in each range correction category was measured. The value of $S(11)$, for example, was equal to the total number of events in which the K^+ decay occurred in S6 and in which the muon deviated from normal incidence on the spark chambers by less than 14.5° divided by the total number of $K^+ \rightarrow \mu^+ + \nu$ events observed. In Table I, $S(j)$ has been divided by 0.964. This constant factor has been combined with other correction factors such as the spark chamber scanning efficiency.

We calculated the background from the decay in flight of π^+ mesons from $K^+ \rightarrow \pi^0 + \pi^+$ in the following manner. We followed a number of pions equal to $\Gamma(K^+ \rightarrow \pi^0 + \pi^+) / \Gamma(K^+ \rightarrow \mu^+ + \nu)$ times the number of scaler counted $K^+ \rightarrow \mu^+ + \nu$ events until they stopped in the degrader region of the spark chamber assembly. We assumed that the attenuation coefficient by nuclear interactions in copper is $1/105$ cm²/g. Since the change in the laboratory trajectory of the charged particle in those $\pi^+ \rightarrow \mu^+ + \nu$ decays in which the muon reached the carbon plates in the stopping region was too small to be observed, the background consisted of all such decays. The total rate of decay per centimeter of path length is $1/\beta\gamma c\tau$, where τ is the pion mean life (25.5×10^{-9} sec). The average component of the polarization in the direction of the pion line of flight of the muons coming to rest at a particular range in the carbon plates is equal to $-\cos\theta$, where θ is the angle in the center-of-mass system between the line of flight of the pion and the direction of the muon. The events from pion decay in flight are assumed to be subject to the same scanning losses and corrections as the $K^+ \rightarrow \pi^0 + \mu^+ + \nu$ events. There is considerable disagreement among the various experimental determinations of the ratio of the $K^+ \rightarrow \pi^0 + \pi^+$

TABLE I. Summary of results. Number of $K^+ \rightarrow \mu^+ + \nu$ events = 166 169. Stopping muon detection efficiency other than $S(j) = 0.876$. d.i.f. = decay in flight.

Range bin	Average energy (MeV)	Events	S	Calculated backgrounds		$K^+ \rightarrow \pi^0 + \pi^+$ d.i.f. Events	$K^+ \rightarrow \mu^+ + \nu$ d.i.f. Events	(Events) - (Background)
				$K^+ \rightarrow \mu^+ + \nu + \gamma$ Events	Polarization			
11	108.5	114	0.484	9.5	-0.97	22.6	0.6	81.3
12	111.25	108	0.888	19.0	-0.97	34.2	0.5	54.3
13	114.0	164	1.000	23.5	-0.98	33.0	0.7	106.8
14	116.75	142	1.000	25.9	-0.98	29.7	0.7	85.7
15	119.5	128	1.000	28.7	-0.98	29.6	0.6	69.1
16	122.25	108	1.000	32.1	-0.99	24.8	0.6	50.5
17	125.0	100	1.000	36.2	-0.99	21.7	0.6	41.5
18	127.75	70	1.000	41.2	-0.99	17.2	0.4	11.2
19	130.5	33	0.498	24.5	-0.99	7.5	0.2	0.8

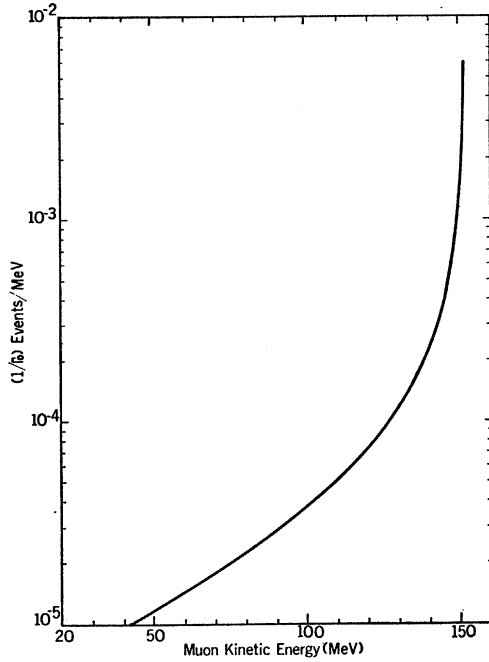


FIG. 4. Energy distribution of μ^+ in the decay $K^+ \rightarrow \mu^+ + \nu + \gamma$. It is assumed that the gamma ray is not detected.

decay rate to the $K^+ \rightarrow \mu^+ + \nu$ decay rate that have been published. In making the above calculations, the value of $[\Gamma(K^+ \rightarrow \pi^0 + \pi^+)]/[\Gamma(K^+ \rightarrow \mu^+ + \nu)]$ has been assumed to be 0.37 ± 0.06 . The assumed error is wide enough to overlap most of the experimental results.⁴

We have calculated the background from the radiative decay $K^+ \rightarrow \mu^+ + \nu + \gamma$ from the matrix element derived by Cabibbo.⁵ This matrix element, in which the so-called structure-dependent effects have been neglected, is

$$M = - (G/\sqrt{2}) M_K f_a (4\pi)^{1/2} e (M_\mu/2 \hat{p}_\mu \cdot \hat{k}) \times \bar{U}_\mu [(\gamma \cdot \epsilon)(\gamma \cdot \hat{k}) + 2 \hat{p}_\mu \cdot \epsilon] (1 + \gamma_5) U_{\nu, \mu}. \quad (4)$$

M_K and M_μ are the K and μ masses, \hat{p}_μ is the muon four-momentum, and ϵ , \hat{k} are the photon polarization and four-momentum. The form factor f_a is defined by M_0 , the matrix element for $K^+ \rightarrow \mu^+ + \nu$.

$$M_0 = - \frac{iG}{\sqrt{2}} M_K f_a \bar{U}_\mu (\gamma \cdot \hat{p}_\mu) (1 + \gamma_5) U_{\nu, \mu}. \quad (5)$$

We computed from these matrix elements the energy distribution and the longitudinal polarization of the muons. We assumed that the γ ray has not been detected. The results are as follows:

⁴ This situation has been clarified in the recently published work of F. Shaklee, C. Jensen, B. Roe, and D. Sinclair, Phys. Rev. 136, B1423 (1964). These authors find the best value for the $(K^+ \rightarrow \pi^0 + \pi^+)/ (K^+ \rightarrow \mu^+ + \nu)$ decay-rate ratio to be 0.356 ± 0.015 .
⁵ N. Cabibbo, Nuovo Cimento 11, 827 (1959).

Muon polarization:

$$P = -B(E_\mu)/A(E_\mu). \quad (6a)$$

Muon energy distribution:

$$d\Gamma(K^+ \rightarrow \mu^+ + \nu + \gamma)/dE_\mu = \Gamma_0 A(E_\mu) (e^2/2\pi P_{\max}^2). \quad (6b)$$

In the above expression, Γ_0 is approximately equal to the observed rate of $K^+ \rightarrow \mu^+ + \nu$. The two functions $A(E_\mu)$ and $B(E_\mu)$ are

$$A(E_\mu) = (E_{\max} - E_\mu) \ln f + \frac{4E_\mu P_{\max}}{E_{\max} - E_\mu} \left(\ln g - \frac{P_\mu}{E_\mu} \right), \quad (7)$$

$$B(E_\mu) = \frac{(E_{\max} - E_\mu)(M_K E_\mu - M_\mu^2) \ln f}{M_K P_\mu} + \frac{4E_\mu(E_{\max} E_\mu - M_\mu^2) \ln g}{P_\mu(E_{\max} - E_\mu)} - \frac{2(E_{\max}^2 + E_\mu^2 - 2M_\mu^2)}{(E_{\max} - E_\mu)}. \quad (8)$$

The functions f and g in the above equations are defined as follows:

$$f = \frac{M_k(E_\mu + P_\mu) - M_\mu^2}{M_k(E_\mu - P_\mu) - M_\mu^2},$$

$$g = (E_\mu + P_\mu)/M_\mu,$$

$$P_{\max} = (M_k^2 - M_\mu^2)/2M_k,$$

$$E_{\max} = (M_k^2 + M_\mu^2)/2M_k.$$

In these expressions E_μ and P_μ are the total energy and momentum of the muon. The units have been chosen such that $e^2 = 1/137$ and $c = 1$. The results of the above calculation are shown in Figs. 4 and 5.

The background from the decay in flight of muons from $K^+ \rightarrow \mu^+ + \nu$ was computed taking into account the muon lifetime, the effect of the T5 anticoincidence

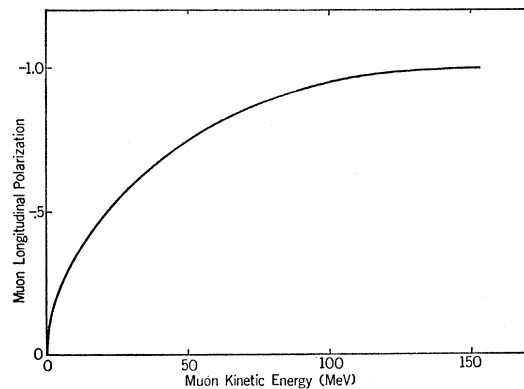


FIG. 5. Longitudinal polarization of μ^+ in the decay $K^+ \rightarrow \mu^+ + \nu + \gamma$. It is assumed that the gamma ray is not detected.

counter, and the annihilation in flight of the decay positrons.

The observed rate for $K^+ \rightarrow \pi^0 + \mu^+ + \nu$ after the above described backgrounds have been subtracted is given in the last column of Table I. In order to make comparisons with various theoretical predictions, it is of interest to determine the rate relative to the total rate for the process $K^+ \rightarrow \pi^0 + e^+ + \nu$. The total number of these events corresponding to the data of Table I has been obtained by multiplying the observed number of $K^+ \rightarrow \mu^+ + \nu$ events by the factor $[\Gamma(K^+ \rightarrow e^+ + \pi^0 + \nu)] / [\Gamma(K^+ \rightarrow \mu^+ + \nu)]$ which has been obtained from a number of experiments.⁶ This factor is taken to be 0.076 ± 0.007 . The results of the rate measurement may be summarized by the following expression:

$$\frac{1}{\Gamma(K^+ \rightarrow \pi^0 + e^+ + \nu)} \times \int_{107.1}^{126.4} \frac{d\Gamma(K^+ \rightarrow \pi^0 + \mu^+ + \nu)}{dE_\mu} S(E_\mu) dE_\mu = 0.044 \pm 0.007.$$

The error takes into account the statistical uncertainties, and the error in determining the muon energy scale. The $S(E_\mu)$ factor is the same as that given in Table I. If the data are corrected for the efficiency function, the results may be expressed as follows:

$$\frac{1}{\Gamma(K^+ \rightarrow \pi^0 + e^+ + \nu)} \int_{107.1}^{126.4} \frac{d\Gamma(K^+ \rightarrow \pi^0 + \mu^+ + \nu)}{dE_\mu} dE_\mu = 0.054 \pm 0.008.$$

The above expression has not been used in the analysis of the data.

B. Muon Longitudinal Polarization Measurement

We measured the polarization of the muons by observing the spatial asymmetry of the decay positrons. The angular distribution of positrons from the decay of polarized muons is

$$W(\theta) = \frac{1}{2} (1 + \frac{1}{3} P \cos\theta). \quad (9)$$

θ is the angle between the muon polarization P and the direction of the decay positron. This formula is correct only if the decay positrons are detected with an efficiency which does not depend on their energy. Since the apparatus used in this experiment was fully sensitive to positrons with an energy greater than 10 MeV, the correction due to the detection efficiency of the apparatus is negligible. In the analysis described here, θ was taken as the angle between the direction of the muon incident on the copper degrader and the direction of the decay positron. This choice reduced the effect of multiple scattering of the muon in the degrader. The

multiple scattering of the muon (15° average) was such that even if the spin remained parallel to the momentum, the apparent attenuation of the polarization would be negligible. Likewise, the uncertainty (15° average) in the measurement of the decay-positron direction had a negligible effect.

The presence of magnetic fields as small as a few gauss appreciably modifies the angular distribution of positrons from the decay of polarized muons. In order to reduce the effect of the stray magnetic field of the Bevatron, the apparatus was placed so that the direction of motion of the muons was parallel to the stray field. At the peak of the magnet current cycle when the Bevatron beam spill occurred, the total magnetic field including that of the earth was less than three gauss, and was within 30° of being parallel to the direction of motion of the muons. The sample of muon decays we used included those from the time of stopping to 3.3×10^{-6} sec thereafter. The reduction of the longitudinal polarization of such a sample under our conditions is less than 2%.

We tested the performance of the apparatus as a polarization analyzer using muons from $K^+ \rightarrow \mu^+ + \nu$ which were brought to rest in the carbon plates. In Fig. 6(a) we show the observed angular distribution of

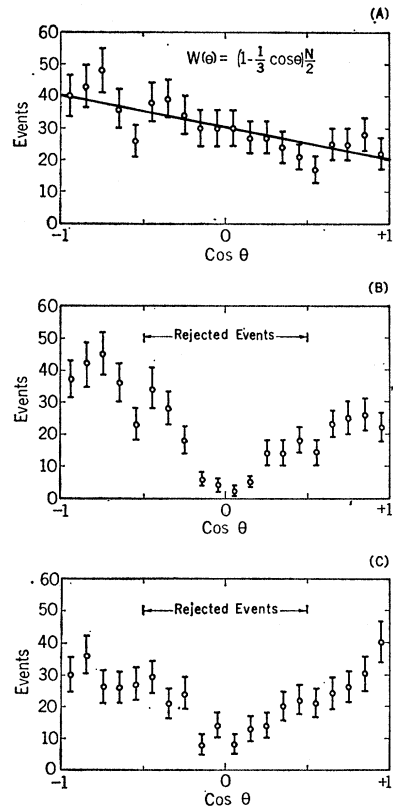


FIG. 6. Angular distribution of positrons from μ^+ decay. (a) Muons from $K^+ \rightarrow \pi^0 + \mu^+ + \nu$ with a minimum positron signature of 1 spark. (b) Muons from $K^+ \rightarrow \pi^0 + \mu^+ + \nu$ with a minimum positron signature of 3 sparks. (c) Muons from background events and $K^+ \rightarrow \pi^0 + \mu^+ + \nu$ with a minimum positron signature of 3 sparks.

⁶ A. Rosenfeld, A. Barbaro-Galtieri, W. H. Barkas, P. L. Astien, J. Kirz, and M. Roos, Rev. Mod. Phys. 36, 977 (1964).

the decay positrons. The solid line is a plot of the distribution expected for 100% negative polarization, i.e., $W(\theta) = \frac{1}{2}N(1 - \frac{1}{3}\cos\theta)$, where N is the total number of events in the sample. In this sample, the minimum signature of a positron from muon decay was a single spark. The $K^+ \rightarrow \pi^0 + \mu^+ + \nu$ experiment was carried out under conditions of a somewhat higher beam rate and occasionally a single, unrelated spark would have been spuriously identified as a positron from a muon decay. In order to eliminate this possibility a minimum of three sparks along the positron track was required. The distribution of the $K^+ \rightarrow \mu^+ + \nu$ events with the three-spark requirement is shown in Fig. 6(b). Evidently the efficiency for detecting muon decays with the positron moving parallel to the spark chamber plates was greatly reduced by this condition. Therefore, in making the polarization analysis, only those events with $\theta < 60^\circ$ and $\theta > 120^\circ$ were used. The three spark condition had only a small effect on the efficiency for observing these events. The polarization computed from these events did not depend on the value chosen for the cutoff angle.

We determined the polarization by a maximum-likelihood analysis. The likelihood,

$$L \propto \prod_j (1 + \frac{1}{3}P \cos\theta_j) \quad (10)$$

has been computed as a function of the assumed polarization P . In this expression, θ_j is the angle between the direction of the positron and the direction of the incident muon for each event. We accepted for analysis only those events with $\theta_j < 60^\circ$ or $\theta_j > 120^\circ$. Figure 7 shows

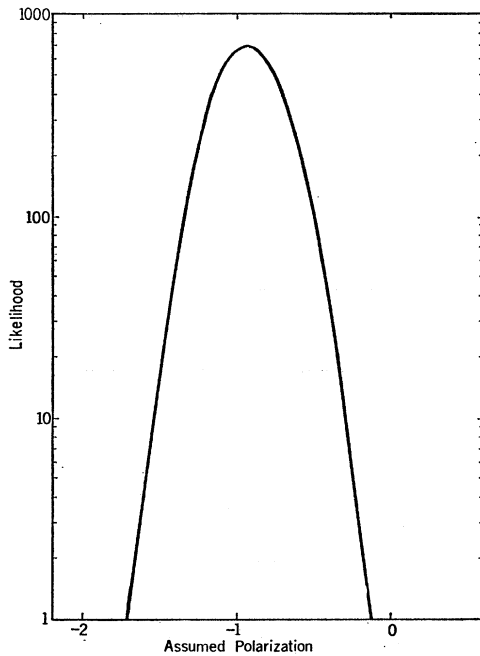


FIG. 7. Likelihood plot for longitudinal polarization of muons in $K^+ \rightarrow \mu^+ + \nu$.

the likelihood L for the polarization of the $K^+ \rightarrow \mu^+ + \nu$ events. The distribution has a mean of -0.94 and a standard deviation of 0.21 . This result is consistent with the result of Coombes *et al.*,⁷ who found $P = -0.93 \pm 0.12$. A muon polarization of -1.0 is expected if the K^+ has zero spin and the neutrino is emitted in a state of complete negative longitudinal polarization.

The angular distribution of the muon-decay positrons in the $K^+ \rightarrow \pi^0 + \mu^+ + \nu$ and background events is shown in Fig. 6(c). The maximum likelihood analysis of this data is shown in Fig. 8. The observed polarization is 0.0 with a standard deviation of 0.22 . The observed polarization must be corrected to account for the large background which is negatively polarized. In the total of 864 events, there was a calculated contamination of 195.6 π^+ decay in flight events, with an average polarization of -0.69 . There were 174.9 $K^+ \rightarrow \mu^+ + \nu + \gamma$ events with an average polarization of -0.98 , and 4.3 μ^+ decay in flight events with an average simulated polarization of 0.0 . In order to account for the fact that the T5 anticoincidence counter rejected forward muon decays within 10^{-8} sec after the muon came to rest, a single event in the forward direction has been added to the above sample. After these corrections, the polarization of the muons from $K^+ \rightarrow \pi^+ + \mu^+ + \nu$ was determined to be $+0.61 \pm 0.39$, i.e.,

$$\frac{\int_{107.1}^{126.4} \frac{d\Gamma(K^+ \rightarrow \pi^0 + \mu^+ + \nu)}{dE_\mu} S(E_\mu) P_\mu dE_\mu}{\int_{107.1}^{126.4} \frac{d\Gamma(K^+ \rightarrow \pi^0 + \mu^+ + \nu)}{dE_\mu} S(E_\mu) dE_\mu} = +0.61 \pm 0.39.$$

DISCUSSION OF RESULTS

In order to interpret these results, a number of assumptions are necessary. We shall assume that the neutrino emitted in the $K^+ \rightarrow \pi^0 + \mu^+ + \nu$ decay is in a state of complete negative longitudinal polarization. The most general local, Lorentz-invariant matrix element not involving derivatives of the fields can be then written as follows⁸⁻¹²:

$$M = \frac{G}{\sqrt{2}} \left\{ \tilde{U}_\mu \left[M_K f_s + i[f_+(P+Q) + f_-(P-Q)] \cdot \gamma \right. \right. \\ \left. \left. + \frac{if_t}{2M_K} (P_a Q_b - P_b Q_a) \sigma_{ab} \right] (1 + \gamma_5) U_{\nu, \mu} \right\}. \quad (11)$$

⁷ C. Coombes, B. Cork, W. Galbraith, G. R. Lambertson, and W. A. Wenzel, *Phys. Rev.* **108**, 1348 (1957).

⁸ J. D. Jackson, *Elementary Particles and Field Theory, 1962 Brandeis Lectures* (W. A. Benjamin, Inc., New York, 1963), Vol. 1.

⁹ J. Werle, *Nucl. Phys.* **6**, 1 (1958).

¹⁰ P. Dennery and H. Primakoff, *Phys. Rev.* **131**, 1334 (1963).

¹¹ N. Brene, L. Egardt, and B. Qvist, *Nucl. Phys.* **22**, 553 (1961).

¹² L. Okun, *Nucl. Phys.* **5**, 455 (1958).

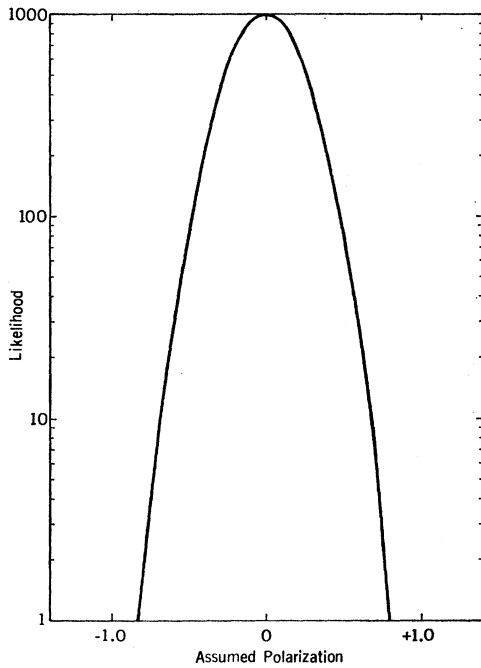


FIG. 8. Likelihood plot for longitudinal polarization of muons in $K^+ \rightarrow \pi^0 + \mu^+ + \nu$ and background events.

In this expression, P is the four-momentum of the K^+ meson, and Q is the four-momentum of the π^0 meson. Each of the form factors (i.e. f_s , f_+ , f_- , and f_t) may be functions of the square of the four-momentum transfer to the muon-neutrino pair, $s = (P - Q)^2$. It will be convenient for the following discussion to make the definition $\xi(s) = f_-(s)/f_+(s)$ for the vector form-factor ratio.

The term in the matrix element proportional to f_- can be recast in the form of a scalar interaction with an effective coupling constant equal to $-M_\mu f_-$. For this reason, there are actually only three independent quantities to be determined. The true scalar interaction differs, however, from the scalar interaction generated by the f_- term in the vector interaction in that the factor M_l ($l = \text{lepton}$) is not present. These two scalar terms thus behave differently under the interchange of muon and electron. In the $K^+ \rightarrow \pi^0 + e^+ + \nu$ decay, the contribution of a f_- term is much smaller than in the $K^+ \rightarrow \pi^0 + \mu^+ + \nu$ decay. It is therefore possible in principle to separate the two types of scalar interaction by comparing the two different decay modes given above.

In the present experiment, the π^0 was not observed. In order to make predictions using the matrix element M , it is therefore necessary to know the momentum-transfer dependence of the form factors. For the remainder of this discussion, we shall assume that they are independent of momentum transfer. Arguments based on a dispersion relation treatment of the form factors indicate that they vary only a small amount

over the region of momentum transfer possible in the $K^+ \rightarrow \pi^0 + \mu^+ + \nu$ decay.¹³

We have computed the longitudinal polarization of the muons as a function of muon energy for pure scalar, vector ($\xi=0$), and tensor couplings. The results are shown in Fig. 9. The polarization we observe is not consistent with a pure scalar or a pure tensor coupling. Furthermore, additional calculations¹⁴ have shown that there is only one combination of scalar and tensor coupling that has a polarization consistent with the experimental result. This combination ($f_t/f_s = 5$, $\delta\theta_{st} = 180^\circ$), however, requires a negative polarization of the muons below a kinetic energy of 95 MeV. There have been two recent experiments^{15,16} in which the muon polarization was observed at kinetic energies in the 70-MeV region. In each experiment, the observed polarization was positive. For this reason it is possible to exclude the scalar tensor mixture as a possible solution. It is therefore necessary that the vector interaction be at least partly responsible for the decay $K^+ \rightarrow \pi^0 + \mu^+ + \nu$.

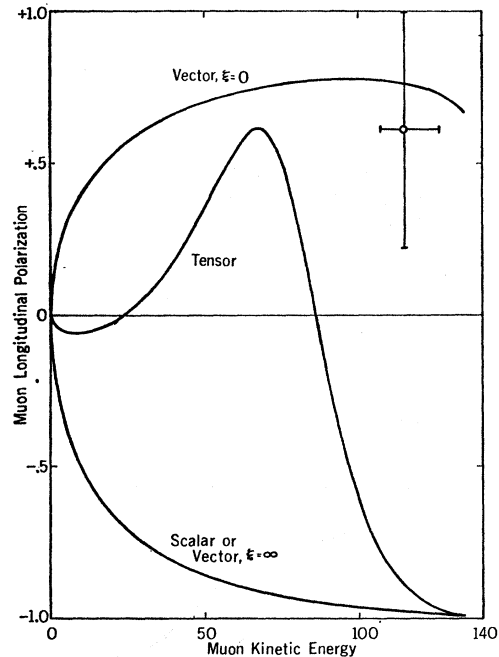


FIG. 9. Longitudinal polarization of muons in $K^+ \rightarrow \pi^0 + \mu^+ + \nu$ for pure scalar, vector ($\xi=0$), and tensor couplings. The polarization for vector coupling with $\xi = \infty$ is identical to that for scalar coupling. The experimental point is not consistent with pure scalar or tensor coupling.

¹³ S. W. MacDowell, Phys. Rev. **116**, 1047 (1959).

¹⁴ We have used the expression derived by Okun (Ref. 12) for this analysis after making the following changes: (1) We assume the expression applies to K^+ decay rather than K^- decay, (2) \bar{A} , \bar{B} , \bar{C} , and \bar{D} are replaced by \bar{A}/M_{K^2} , \bar{B}/M_{K^2} , \bar{C}/M_K , and \bar{D}/M_K , and (3) the interference terms f_{sv} , f_{st} , and f_{vt} have been multiplied by 2.

¹⁵ V. Smirnitski and A. Weissenberg, Phys. Rev. Letters **12**, 233 (1964).

¹⁶ G. Gidal, W. M. Powell, R. March, and S. Natali, Phys. Rev. Letters **13**, 95 (1964).

For the remainder of the discussion we shall assume that the interaction is of a pure vector type and that the form factors are constant. Assuming this, the matrix element for the decay is

$$M = C_\mu \{ \bar{U}_\mu [(P+Q) + \xi(P-Q)] \cdot \gamma (1 + \gamma_5) U_{\nu, \mu} \}. \quad (12)$$

In the above expression C_μ is a constant. The above matrix element leads to a component of muon polarization out of the plane of the decay proportional to the imaginary part of ξ . Hence, the assumption of time reversal invariance would require that ξ be real. Recent experimental results on K_2^0 decay have indicated that time reversal invariance may be violated.¹⁷ For this reason, we shall not assume ξ is real in the present discussion.

For comparison with the experimental polarization measurement, the following function has been computed from the above matrix element.

$$P(E_\mu)_{av} = \frac{\int_{107.1}^{126.4} \frac{d\Gamma(K^+ \rightarrow \pi^0 + \mu^+ + \nu)}{dE_\mu} S(E_\mu) P(E_\mu) dE_\mu}{\int_{107.1}^{126.4} \frac{d\Gamma(K^+ \rightarrow \pi^0 + \mu^+ + \nu)}{dE_\mu} S(E_\mu) dE_\mu}. \quad (13)$$

In the above expression, $S(E_\mu)$ is the energy-dependent detection efficiency given in Table I, and $P(E_\mu)$ is the muon longitudinal polarization. The above expression depends only on ξ being independent of the constant factor C_μ . The result of this calculation is shown in Fig. 10. If ξ is real, the experimental result requires that $-4.0 < \xi < +1.7$. We have used the expressions derived by Dennery and Primakoff¹⁰ and by Brene, Egardt, and Qvist¹¹ in the above analysis.

In order to calculate the absolute rate of $K^+ \rightarrow \pi^0 + \mu^+ + \nu$ decay, it is necessary to know the value of the con-

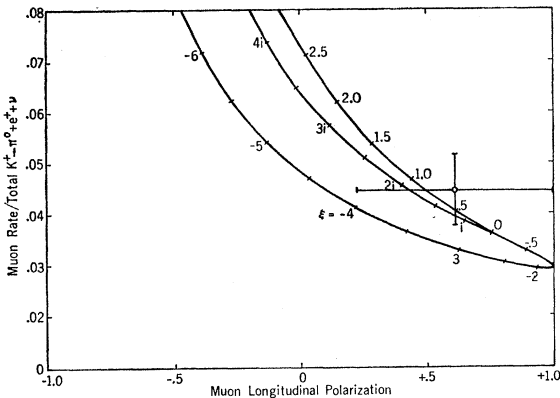


FIG. 10. Muon longitudinal polarization and energy spectrum assuming pure vector coupling, constant form factors, and equal muon and electron coupling strengths. The curve is the locus of points with varying vector form-factor ratio ξ .

¹⁷ J. N. Christenson, J. W. Cronin, V. L. Fitch, and R. Turlay, Phys. Rev. Letters 13, 138 (1964).

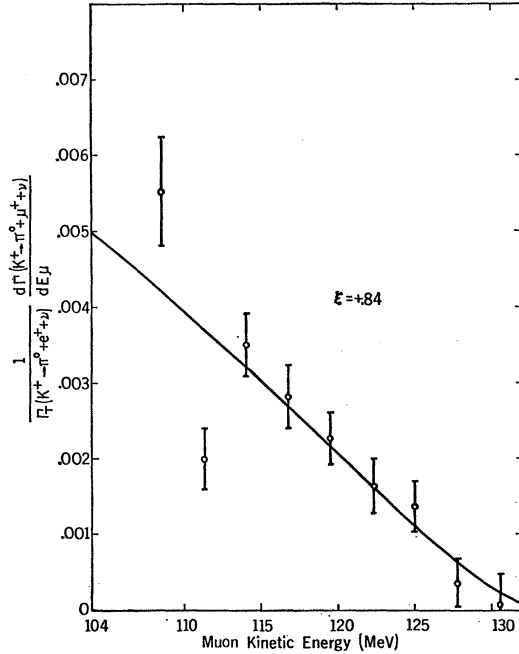


FIG. 11. Energy distribution of muon in $K^+ \rightarrow \pi^0 + \mu^+ + \nu$. The experimental points have been corrected to account for backgrounds and the varying detection efficiency.

stant C_μ as well as the value of ξ . By making the assumption that the weak coupling strength of muons is the same as that of electrons, it is possible to determine C_μ from the observed rate of $K^+ \rightarrow \pi^0 + e^+ + \nu$ decay. This assumption is equivalent to the statement that the matrix element used for the computation of the $K^+ \rightarrow \pi^0 + e^+ + \nu$ decay is the same as that used for the computation of the $K^+ \rightarrow \pi^0 + \mu^+ + \nu$ decay except that m_e is substituted for m_μ wherever the lepton mass appears. Making this assumption, we have computed the ratio of the rate at which muons from $K^+ \rightarrow \pi^0 + \mu^+ + \nu$ stopped in our apparatus to the total rate of $K^+ \rightarrow \pi^0 + e^+ + \nu$ decay.

$$\text{Rate} = \frac{\int_{107.1}^{126.4} \frac{d\Gamma(K^+ \rightarrow \pi + \mu^+ + \nu)}{dE_\mu} S(E_\mu) dE_\mu}{\int_0^{E_{\max}} \frac{d\Gamma(K^+ \rightarrow \pi^0 + e^+ + \nu)}{dE_e} dE_e}. \quad (14)$$

This function depends only on ξ . The result of this calculation is shown in Fig. 10. If ξ is real, the observed decay rate implies that $+0.2 < \xi < +1.4$ or $-4.8 < \xi < -3.5$.

In Fig. 10 we have combined the results and the theoretical predictions for the muon polarization and decay rate. The solution with $+0.2 < \xi < +1.4$ is evidently the most probable provided that ξ is real. Solutions with ξ imaginary, as suggested by Cabibbo,¹⁸

¹⁸ N. Cabibbo, Phys. Letters 12, 137 (1964).

are also possible. In that case, the results imply that $0.8 < |\xi| < 2.6$. It is important to note that the experimental point in Fig. 10 is consistent with at least one value of ξ . If the muon weak-coupling strength C_μ were appreciably different from the electron weak coupling strength C_e , the experimental result would not be consistent with any value of ξ . In order that the experimental result be consistent with at least one value of ξ , it is necessary that $0.77 < |C_\mu|/|C_e| < 1.48$.

The ratio of the differential muon spectrum in $K^+ \rightarrow \pi^0 + \mu^+ + \nu$ to the total rate of $K^+ \rightarrow \pi^0 + e^+ + \nu$ has been computed for $\xi = +0.84$. The computation and the experimental results corrected for the detection efficiency are shown in Fig. 11.

The $K^+ \rightarrow \pi^0 + \mu^+ + \nu$ decay has been investigated in a number of experiments. The results of the present experiment are consistent with the results of the experiments of Gidal *et al.*,¹⁶ Smirnitski and Weissenberg,¹⁵ Jensen *et al.*,¹⁹ and Brown *et al.*²⁰ Our results are not in agreement with various aspects of the experiments of Dobbs *et al.*²¹ and Boyarski *et al.*²²

¹⁹ G. L. Jensen, F. S. Shaklee, B. P. Roe, and D. Sinclair, Phys. Rev. **136**, B1431 (1964).

²⁰ J. L. Brown, J. A. Kadyk, G. H. Trilling, R. T. Van de Walle, B. P. Roe, and D. Sinclair, Phys. Rev. Letters **8**, 450 (1962).

²¹ J. M. Dobbs, K. Lande, A. K. Mann, K. Reibel, F. J. Sciulli,

SUMMARY

An analysis assuming a pure vector interaction with constant form factors and equal muon and electron weak-coupling strength has been shown to be consistent with the experimental observations. The vector form-factor ratio ξ can be real or imaginary. The probable solutions for ξ are shown in Fig. 10. There is no evidence on the basis of the present experiment that the form of the leptonic weak-interaction current J_λ^l in the coupling to the current of the strongly interacting particles which changes strangeness $J_\lambda^{s, \Delta s=1}$ is different from the form of J_λ^l in the coupling to the currents which do not change strangeness.

ACKNOWLEDGMENTS

We wish to thank Professor E. Segrè for his advice and encouragement, and Dr. N. Cabibbo and Dr. W. Chinowsky for many helpful discussions. Many of the calculations were made by A. Maksymowicz. The Bevatron operation was under the supervision of W. Hartsough.

H. Uto, D. H. White, and K. K. Young, Phys. Rev. Letters **8**, 295 (1962).

²² A. M. Boyarski, E. C. Loh, L. Q. Niemela, D. M. Ritson, R. Weinstein, and S. Ozaki, Phys. Rev. **128**, 2398 (1962).

Solution of the Schrödinger Equation with a Hamiltonian Periodic in Time*

JON H. SHIRLEY†

California Institute of Technology, Pasadena, California

(Received 8 November 1963; revised manuscript received 18 January 1965)

The interaction of a quantum system with an oscillating field is studied in a formalism which replaces the semiclassical time-dependent Hamiltonian with a time-independent Hamiltonian represented by an infinite matrix. The formalism is developed as a mathematical equivalent to the semiclassical treatment, and interpreted as a classical approximation to the quantum treatment of the field. Combined with a perturbation theory for two nearly degenerate states, the formalism provides a convenient method for determining resonance transition probabilities including frequency shifts and multiple quantum transitions. The theory is illustrated by a detailed study of the simple case of a two-state system excited by a strong oscillating field.

I. INTRODUCTION

CONSIDER a quantum system with two discrete states α and β . Let the amplitudes for the system to be in these states be $a_\alpha(t)$ and $a_\beta(t)$; the energies, E_α and E_β . Let an oscillating interaction connect these states with a matrix element $2b \cos \omega t$, where b is real. Then the system evolves according to the Schrödinger

equation ($\hbar=1$)

$$i \frac{d}{dt} \begin{pmatrix} a_\alpha(t) \\ a_\beta(t) \end{pmatrix} = \begin{pmatrix} E_\alpha & 2b \cos \omega t \\ 2b \cos \omega t & E_\beta \end{pmatrix} \begin{pmatrix} a_\alpha(t) \\ a_\beta(t) \end{pmatrix}. \quad (1)$$

If at some initial time t_0 the system is in state α , then $|a_\beta(t)|^2$ represents the transition probability to state β , and is a function of t , t_0 , b , ω , and the energy separation $E_\alpha - E_\beta$. A physical example of this simple system is a spin one-half particle in a static magnetic field with an oscillating magnetic field at frequency ω applied perpendicular to the static field.

* Based on a thesis submitted to the California Institute of Technology in partial fulfillment of the requirements for the degree of Doctor of Philosophy.

† Present address: National Bureau of Standards, Radio Standards Laboratory, Boulder, Colorado.